

## Design of A Conformal Fractal Antenna with SIW for Medical Implants Application

**Abstract** This paper proposed a new design of fractal antenna with Substrate Integrated Waveguide (SIW) and dual-resonant for wireless implantable capsule systems. The proposed antenna conforms to an implantable capsule with an 11 mm radius and 25 mm length without occupying the capsule's internal space. The proposed antenna has four slots and a fractal shape for extending the effective current path. The substrate is using Rogers 5880, with 2.2 as relative permittivity and 0.787 mm thickness, while the capsule is made of medical Teflon plastic. This proposed design achieves conformal characteristics with human tissue compatibility. Computer simulation technology (CST) software was used to simulate and analyze the antenna in different variety of environments. At operating frequency of 2.4 GHz and 5.8 GHz industrial, scientific and medical (ISM). The antenna's bandwidth reach (2.1 GHz-2.3 GHz) and (5.42 GHz-6.04 GHz). The maximum gains of -7.5 dBi and -5.1 dBi at 5.8 GHz and 2.4 GHz, respectively. Voltage standing wave ratio (VSWR) of 1.2 and 1.17, and front-to-back ratio (FBR) of 20.4 dB and 16.07 at 5.8 GHz and 2.4 GHz, respectively. The antenna was experimentally measured in a minced pork. From the result and analysis, it is confirmed that the proposed antenna is successfully suited for wireless implantable capsule systems.

**Streszczenie.** W tym artykule zaproponowano nowy projekt anteny fraktalnej z falowodem zintegrowanym z podłożem (SIW) i podwójnym rezonansiem dla bezprzewodowych systemów wszczepialnych kapsułek. Proponowana antena odpowiada wszczepialnej kapsułce o promieniu 11 mm i długości 25 mm bez zajmowania wewnętrznej przestrzeni kapsułki. proponowana antena ma cztery szczeliny i kształt fraktalny do wydłużenia skutecznej ścieżki prądu. Podłoże wykorzystuje Rogers 5880, o przenikalności względnej 2,2 i grubości 0,787 mm, podczas gdy kapsułka jest wykonana z medycznego teflonu. Ten proponowany projekt osiąga cechy zgodne z kompatybilnością tkanek ludzkich. Do symulacji i analizy anteny w różnych środowiskach wykorzystano oprogramowanie technologii symulacji komputerowej (CST). Przy częstotliwości roboczej 2,4 GHz i 5,8 GHz dla zastosowań przemysłowych, naukowych i medycznych (ISM). Zasięg pasma anteny (2,1 GHz-2,3 GHz) i (5,42 GHz-6,04 GHz). Maksymalne zyski -7,5 dBi i -5,1 dBi odpowiednio przy 5,8 GHz i 2,4 GHz. Współczynnik fali stojącej napięcia (VSWR) 1,2 i 1,17 oraz stosunek przód-tył (FBR) 20,4 dB i 16,07 odpowiednio przy 5,8 GHz i 2,4 GHz. Antenę mierzono eksperymentalnie w mielonej wieprzowinie. Na podstawie wyników i analiz potwierdzono, że proponowana antena z powodzeniem nadaje się do bezprzewodowych systemów wszczepialnych kapsułek. (**Projekt konformalnej anteny fraktalnej z SIW do zastosowań w implantach medycznych**)

**Keywords:** Implantable Antenna, Capsule Antenna, Specific Absorption Rate (SAR).

**Słowa kluczowe:** antena wszczepiana, antena kapsułkowa, specyficzny współczynnik absorpcji (SAR).

### I. Introduction

Nowadays, wireless technology is currently commonly employed in implantable medical devices since it removes the restrictions of wired devices from the body [1]. Implantable devices, such as capsule endoscopes [2], cardiac human body for auxiliary therapy pacemakers [3], and intracranial pressure monitoring, have been inserted into many diseases recently [4].

With the advancements in medical technologies, the requirement for real-time video transmission has outpaced the demand for simple images [5], [6]. Also, the wideband transmission antenna must be created to fulfil the transmission demands of the implanted capsule system so that video and other signals of big data can be transmitted in real-time. Furthermore, the implanted antenna must be wideband for adapting to complicated implanted environments and enhance the antenna's robustness [7]. An implanted system's life cycle must be as long as feasible because of the requirements for the high rates of data transfer [8].

The antenna might be multi-frequency or dual-frequency for extending the battery life [9]. Features, so that a system in a dual-mode working properties. As a result, developing a broadband and dual-frequency implanted antenna offers significant scientific value. A high-dielectric substrate, spiral patch, and open-end ground slot have been utilized in [10] for achieving multi-frequency at 1.6 GHz, 402 MHz, and 2.4 GHz, with 219 MHz as a maximum bandwidth. Despite the fact that such design has multi-

frequency characteristics, the bandwidth is very small, which occupies the space in the implantable device types. Through the addition of a shorting pin, open-ended ground slot, as well as hexagonal and T-shape slots in a radiator, the suggested antenna is developed to function in 2.45 GHz and 915 MHz with a bandwidth of 560 MHz and 107.5 MHz in [11].

Although the device's bandwidth might be expanded, the device's complicated structure causes an increase in the device's dimensions. Even though multi-band or dual-band properties are achieved in [12]. the difficulties of narrow bandwidth, as well as large internal space, took up persist. Because of the limited space available in implantable devices, maintaining antenna broadband and dual-band, whereas lowering antenna's space is a high priority. To save space, certain miniaturization approaches are utilized, including high dielectric constant substrates, meandering lines [13],[14] spiral lines [15], opening slots [16] and the addition of shorting pins and stacking antennas [17]. Yet, such miniaturization technologies frequently cause issues in the antenna design and production process, as well as occupying limited space. Conformal might enhance miniaturization performance when put to comparison to using miniaturization. Also, the conformal structure might efficiently use the capsule's surface to avoid competing for important space with electronic elements in a capsule [18]. Even though the proposed antennas might be conformal with the flexible material types, their efficiency

has failed to attain wide-band and multi-band performance, as shown in research [19].

Depending on the preceding literature, designing a conformal antenna with dual-band properties while reducing contact area with the internal circuit has been considered as an issue worth considering. Given that the internal structure of the wireless implantable capsule is changed, it has the potential to be employed as a cardiac pacemaker in the heart and a capsule speculum in the digestive system. The suggested antenna's operating band can be between 2.42- 2.48 GHz and 5.725-5.850 GHz, which are both in the scientific, industrial, and medical (ISM) frequency bands [20].

A wireless implantable capsule system with a dual-band fractal antenna and substrate integrated waveguide (SIW) is examined in this technique. It has been confirmed to be a wireless implantable capsule system that has a 11 x 25 mm size. The dielectric is Rogers 5880 with thickness of 0.787 mm, relative permittivity of 2.2 and loss tangent of 0.008. Voxel models has been adapter for implanting the antenna into the human body, Gustav was chosen, and experiments were used to assure safety. The assessed materials environment to simulate the human body was minced pork. Considerable results have been achieved.

## II. Design and analysis of antenna

### A. Antenna design process

Figure 1 displays the antenna in a planar view prior to being wrapped. It includes a meandering fractal antenna with a SIW structure. As Figure 1 shows, firstly to design a flat patch antenna with appropriate dimensions in order to bend it and insert it inside the Teflon capsule. The main problem is that there is no meaning for simulating the design with a flat shape (if the design will be bend in the next step). Although, there is no easy method to design the antenna in bending shape directly. So, the design should be started from flat then converted to bending shape, and to do any optimizing work, the research has to return back to the flatten design.

The SIW structure is distributed in the patch and optimized, each hole, D has 0.5 mm as a diameter, and the distance between the vias, S1 is 1 mm., Furthermore, the capsule antenna's substrate is Rogers 5880 (tangent of loss 0.0009, relative permittivity 2.2), which is a conformal. Also, the metal conductor on the substrate's surface is with 0.035 mm thickness of copper, before being wrapped as well as inserted into a capsule shell. The antenna port should be welded using a 50Ω, thick coaxial cable by assuming the z-axis direction capsule. The simulation setup of the proposed capsule antenna is in CST. The capsule antenna is also situated at the model's centre, unless otherwise specified. Table 1 lists the detailed parameters for the designed antenna.

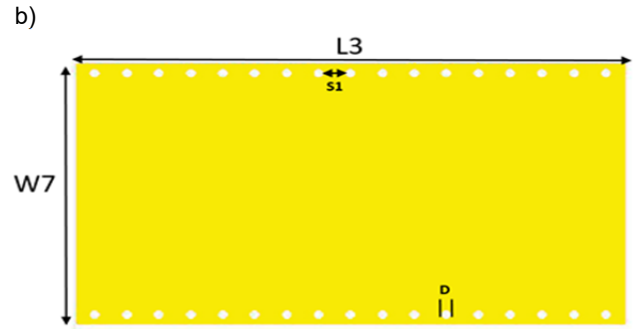
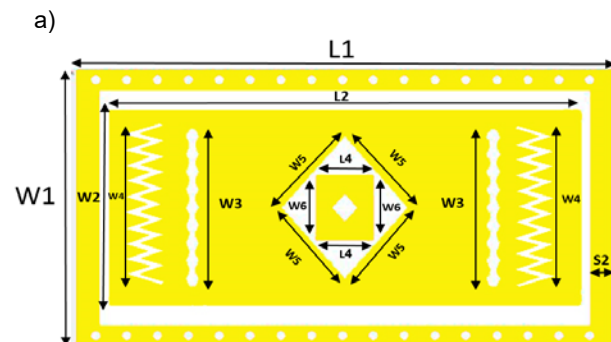


Fig. 1. The proposed fractal antenna with SIW; (a) before bend, (b) reflector layer.

Table 1. Dimensions of the proposed antenna

Parameter	Dimension (mm)	Parameter	Dimension (mm)
L1	31.5	W1	15.00
L2	30.40	W2	10.00
L3	11.50	W3	7.50
L4	8.40	W4	7.00
W6	3.00	W5	4.90
S1	1.05	W7	15.00
S2	2.00		
D	0.5		

Figure 2 displays the capsule design, the outer dimension of the cap. is 11 mm, the inner diameter is 10.4 mm, the cylinder part is 14 mm in length and the total capsule length with a half-spherical shape (in each end) is 25 mm. The capsule should be made from hard Teflon with length of 25 mm and outer diameter and inner diameter of 11 mm and 10.4 mm, respectively. A hole should be made with a diameter of 2.5 mm near the end of the linear part with a distance of approximately 1 mm from the dead end. It is important to know that the inner thickness of the capsule is very important and the outer can be reached up to 0.5 mm. The proposed antenna wrapped around a foam sponge of 10 mm diameter, while its dielectric property is close to that of air, making it negligible.. In addition, the substrate will be 1 mm shorter, and the two feeding vias, denoted by the feeding points in the figure, are situated at the substrate's top edges. In the case when the substrate is wrapped, both vias become 1 mm apart, and they are soldered to the coaxial cable's central core and metallic shield, respectively. By creating the antenna in this way, the soldering of copper strips that form a loop is avoided. In addition, in practical implementations, the coaxial cable must be linked to the capsule's cable. In this studies, a hole is drilled in the capsule cap for allowing the coaxial cable to pass through and connect to a vector network analyzer (VNA) in order to assess the impedance-matching characteristic of the produced capsule antenna. Table 2 lists the detailed proposed capsule structure.

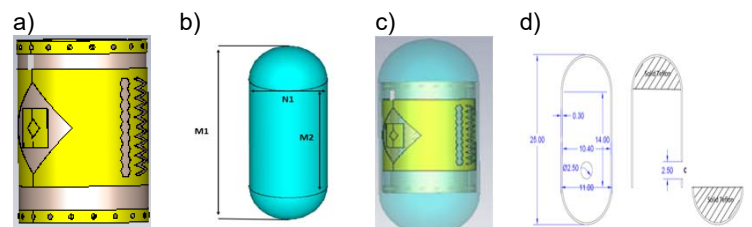


Fig. 2. The proposed fractal antenna with SIW after bending; (a) capsule structure, (b), and (c) proposed capsule antenna, (d) and capsule structure with demission.

Table 2 lists the detailed proposed capsule structure.

Parameter	Dimension (mm)
M 1	25.00
M 2	14
N 1	11

## B. The simulation environment

Since the antenna is impacted via a comparatively high permittivity of the human tissues that tend to cost-effectively miniaturize the antenna's physical size, wave-length in the human body has been found short compared to that in free space [21]. For simulating various working settings, a simple set of human body voxel models was created. Table 3 lists the electromagnetic characteristics of human tissues in different parts [22].

TABLE 3. Dielectric properties of biological tissues at 2.4 GHz and 5.8 GHz [22].

Tissue type	2.4 GHz		5.8 GHz	
	$\epsilon_R(F/m)$	$\delta (S/m)$	$\epsilon_R(F/m)$	$\delta (S/m)$
Muscle	52.791	1.705	48.485	4.962
Fat	5.285	0.102	4.955	0.293
Mucous Membrane	42.923	1.5618	38.624	4.342

## C. Parametertstudy and discussion

As can be seen in Figure 3, the antenna is implanted in the human body voxel models simulation model. This work indicates that various parts of the antenna excite resonance at many frequency values based on the effective current distributions of the antenna at 2.4 GHz and 5.8 GHz as depicted in Figure 4. This work examines a few key antenna structure parameters. To begin with, the antenna is mostly dependent on fractal shape radiation; thus, the proposed antenna's two slots with zigzag shape and two slots with zigzag and shape Hexagon [23], [24]. The parameter two zigzag shape slot have an important impact on the antenna's performance in Figure 4, multi numbers of zigzag shapes and slot width were examined to shift the center frequency ,where the hexagon enhanced the S11 value while the fractal shape enhanced the bandwidth.



Fig 3. Anatomical voxel model Gustav [25].

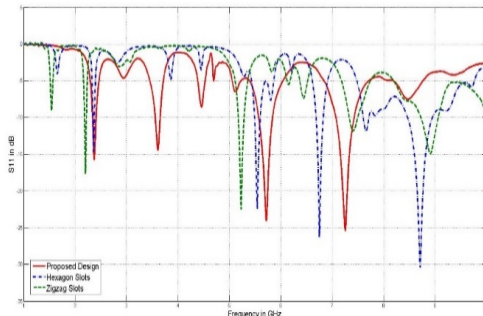


Fig. 4. Simulated  $|S_{11}|$  proposed antenna compared with Zigzag slot and Hexagon slot. It explains the parameter study of  $s_{11}$  and explains all the effects in our design. No need for citation because I don't have a low design and need to be compared. Just justify how it was obtained. The  $s_{11}$  parameter.

## D. Simulations with the complex human models

The human body is a complicated structure made up of a variety of organs, tissues, and bone structures with diverse geometries. The parts of the human body, like legs, arms, and torso are made up of three tissue types: skin, fat, and muscle approximated for simplifying the physical and geometrical qualities of an anatomical model. The research depends on a basic three-layered tissue model (muscle, fat, and skin). The bone layers have been left out of experimental and numerical research for a variety of reasons. The implanted devices utilized for the delivery of medications, like insulin, for instance, are usually positioned in soft human tissue to create a network between sensors [26]. Furthermore, in a few human body parts, the bone serves as the inner layer. The muscles attenuate the laterally sent signals, and they hardly reach the bone. The three-layered tissue model's extraction procedure is shown in Figure 5. The presence of fat tissue around the model is widespread, as is the presence of fat tissue surrounding all of the main human body organs. The three-layered tissue model (skin-fat-muscle) anatomical voxel models, Gustav has been selected. As illustrated in Figure 5, after that, as can be seen in Figure 6, we compared the  $|S_{11}|$  in a simple and complex environment. Based on the findings, the proposed antenna can perform in a variety of environments because of the antenna structure's stability as a possibility for implantable medical devices (IMDs).

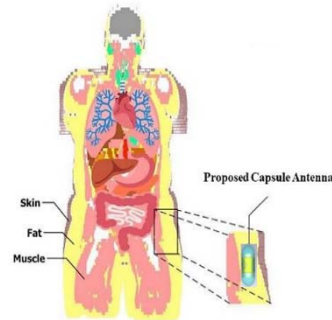


Fig. 5. The environment of the proposed system is a capsule working in the human body.

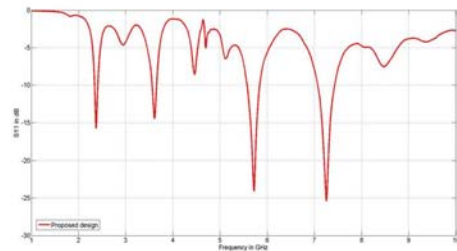


Fig. 6. Simulated  $|S_{11}|$  proposed antenna

## III. Radiation performance evaluation

### A. Radiation performance at different orientations

The proposed antenna is going to be experimented and investigated in various settings at 2.4 GHz and 5.8 GHz. At 2.4 GHz radiation patterns, the antenna radiation pattern is modified by adjusting the direction angle to 90° degrees. The gain is -7.5 dB and -5.2.1dBi at 2.4GHz and 5.8 GHz, respectively. It can be seen as in Figure 7 of the radiation pattern of (a) H-plane and (b) E-plane. At 5.8 GHz and 2.4 GHz, peak radiation efficiencies are 1.33% and 1.18%, respectively. As a result, high-quality antenna performance may be guaranteed at various capsule orientation values in the body.

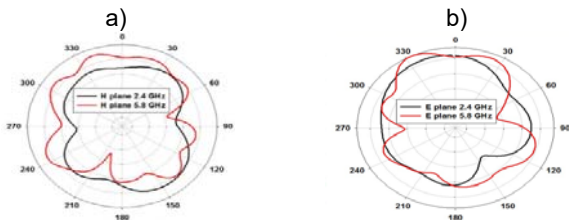


Fig. 7. The radiation pattern of the proposed antenna; (a) E-plane and (b) H-plane.

### B. The SAR of System

The safety concern of implantable antenna must be taken into account. Specific absorption rate (SAR) has been commonly indicated as a criterion of the evaluation for implantable antenna, the levels of the SAR averaged over 1g of the human tissues must be not more than 1.6 W/kg [27]. The antenna's SAR in several models of the simulation at 2.4GHz is shown in Figure 8(a). At 5.8 GHz, Figure 8(b) shows the antenna's SAR in several simulation models. The simulation models that are displayed in Figure 8 is where the case with input power has of 1 W. When the antenna's SAR is smaller than 1.6 W/kg, one might compute the maximal input power of the antenna in a heart simulation model and large intestine simulation model at 5.8GHz and 2.4GHz, respectively. Table III (there is no table III) shows SAR and maximum input power that can be used. Table 4 shows the comparisons of the proposed antenna with suggested antennas in prior works. The proposed antenna obtained dual-band and conformity as compared to other multi-band or dual-band antennas. The SIW manage to decrease the value of SAR.

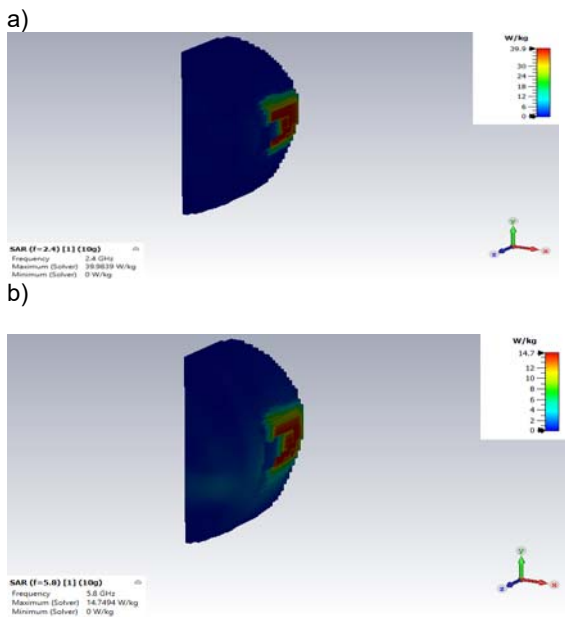


Fig. 8. The simulation average SAR distribution over 10 g for (a) at 2.4GHz, (b) at 5.8GHz.

### C. The gain of the proposed antenna

The simulated gain of the proposed antenna inside the body is depicted as in Figure 9 with SIW and without SIW. It indicates that the maximum gain achieved -7.5 dB and -5.1 dB at 5.8 GHz and 2.4 GHz, respectively. The proposed antenna with SIW successfully shown it has increased gain.

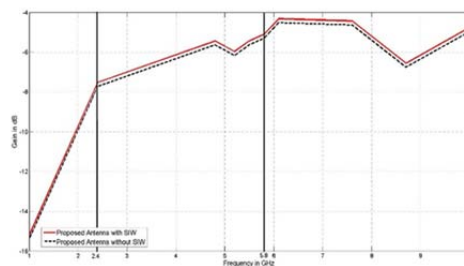


Fig. 9. The Simulated Gain of the Proposed Antenna with and without SIW

### D. Front-To-Back Ratio (FBR) Of The Proposed Antenna

Figure 10 shows the measured frequency dependence of the front-to-back ratio, which always exceeds the level of 20 dB for 2.4 GHz, and achieve 16dB for 5.8 GHz. The proposed antenna with SIW also prove that it manages to increase the front-to-back ratio.

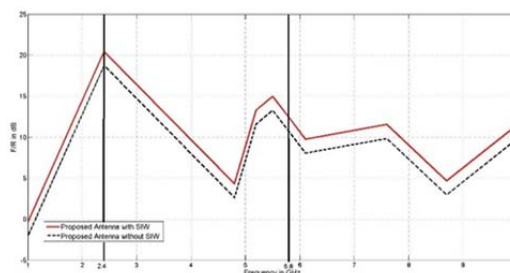


Fig. 10 The simulated front-to-back ratio (FBR) of the proposed antenna

## IV. Measurement results analysis

The antenna developed based on Tables 1,2 evaluated in minced pork, is shown in, Figure 11. Return Loss (dB) can be characterized as an incoming signal ratio to the same reflected signal when it gets into a component that is associated with the parameters of the scattering. The proposed antenna has been anticipated for operating in ISM (2.4–5.8 GHz) band The antenna includes a capsule shell. the performance of the designed antenna structure. The measured and the simulated  $|S_{11}|$  of the antenna in the minced pork is shown in Figure 12, and the result reveals that the antenna's working might cover 2.42 GHz-2.48 GHz and 5.725 GHz-5.85 GHz in various conditions.



Fig 11. Photographs of the Fabrication proposed fractal capsule Antenna.

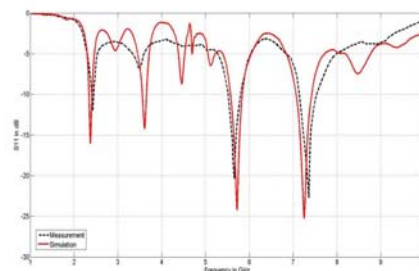


Fig. 12. Simulated and measured  $|S_{11}|$  of proposed capsule antenna.

Figure 11 shows a comparison of the voxel model's measured and simulated radiation patterns. Figures 13 exhibits a comparison of the results of the simulation and real radiation pattern measurements in the case where the antenna is operated at 5.8GHz and 2.4GHz, respectively. The antenna has sufficient radiation properties in an

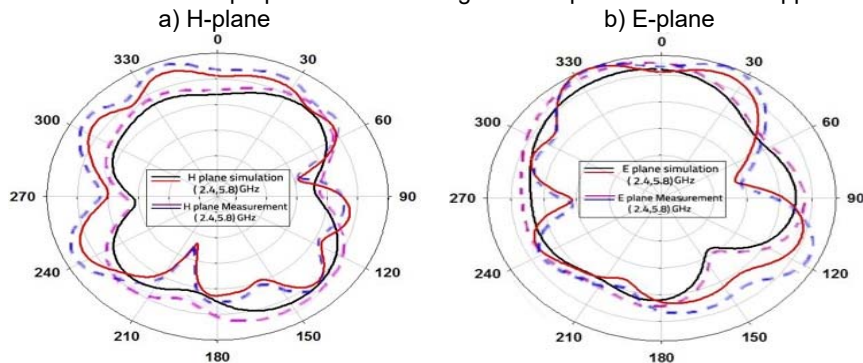


Fig. 13. Comparison of the simulated and measured radiation patterns.

Table 4. Comparison of reported capsule antennas with the proposed antenna in this work

Ref	Year	Frequency operation	Dimension (mm <sup>3</sup> )	Substrate	$\epsilon_r$	Thickness (mm)	Depth (mm)	Gain (dBi)	SAR (W/kg)	Antenna type
[28]	2014	2.4GHz	10 × 10 × 1.27	Rogers 3010	10.2	0.635	4 skin	-22	213	Conformal
[29]	2014	2.4GHz	10 × 5.5 × 3.81	Rogers 3010	10.2	0.635	50 muscle	-32	599	Conformal
[30]	2016	2.4GHz	10 × 10 × 1.27	Rogers 3010	10.2	0.635	5 muscle	-22.33	350	Conformal
[31]	2017	2.4GHz	8.5 × 8.5 × 1.27	Rogers 3010	10.2	0.635	4 skin	-27	200	Embedded
[32]	2017	915 MHz	15 × 15 × 1.27	Rogers 3010	10.2	0.635	3 skin	-32	517	Embedded
[33]	2018	915 MHz	11 × 11 × 1.27	Rogers 3010	10.2	0.635	4 skin	-29	N/A	Conformal
[34]	2019	402–405 MHz	7 × 6.5 × 0.377	Rogers 6010	9.8	0.2	3 skin	-30.22	66	Embedded
[35]	2020	402 915 1200	10 × 10 × 1.27	Rogers ULTRALAM	2.9	0.1	5 muscle	-30.8 -19.7 -18.7	60.9 53.9 50.5	Conformal
[36]	2020	2.4GHz	22 × 23 × 1.27	Rogers 6010	10.2	1.2	3 skin	-36	64	Embedded
[37]	2021	2.4GHz	25 × 25 × 1.28	Rogers 3210	10.2	0.25	3 skin	-18.33	36	Conformal
<b>This Work</b>	<b>2022</b>	<b>2.4 GHz 5.8 GHz</b>	<b>11 × 25 × 1.28</b>	<b>Rogers 5880</b>	<b>2.20</b>	<b>0.787</b>	<b>5 muscle</b>	<b>-7.5 -5.1</b>	<b>39.9 14.7</b>	<b>Conformal</b>

## V. Conclusion

The miniaturized implantable antenna which may be utilized as for medical implants application is designed using a fractal SIW antenna structure and conformal features of capsule shell. At 2.4 GHz and 5.8 GHz, the Dual-band functionality is used. The effect of the proposed antenna's structure on the antenna is investigated using the simple voxel model Gustav model that has been constructed. The minced pork models are used to represent the antenna's actual working environment. For simulation, the research of SAR verifies safety regarding the proposed antenna to the patients by following IEEE C95.1-1999 criteria [38]. When put to comparison to previously proposed dual-band implanted antennas, the proposed antenna stands out and shows a promising better performance. To ensure that the antenna design was feasible, the measured results in minced pork is benchmarked with the simulated data. Lastly, the aim is for the results to be beneficial as references for the designers who are engaged in developing a similar type of capsule for the implant antenna.

## Acknowledgment

The authors would like to thank all who contributed toward making this research successful. The authors wish to express their gratitude to Ministry of Higher Education (MOHE) (Fundamental Research Grant Scheme with reference no: FRGS/1/2020/TK0/UTM/02/64 or R.J130000.7851.5F296), Research Management Center

environment of simulation and measurements, depending on the comparison results. The comparison with the proposed antennas in the previous work is displayed in Table 4. Compared with other dual-band or multi-band antennas, the proposed antenna achieved the acceptable gain for implantable antenna application.

(RMC), Universiti Teknologi Malaysia for the financial support and advice for this project (UTM TDR Grant with reference no: Q.J130000.3551.06G63 and UTMFR Grant with reference no Q.J130000.2551.21H64).

**Authors:** Mustafa Mohammed Jawad, School of Electrical Engineering, Universiti Teknologi Malaysia, Johor Bahru, Malaysia, Email: mustafa.utem@gmail.com; Dr. Nik Noordini Nik Abd Malik, School of Electrical Engineering, Universiti Teknologi Malaysia, Johor Bahru, Malaysia, Email: noordini@utm.my; Alia Jassim Mohammed, Department of Medical Instrumentation Engineering Techniques, College of Medical Techniques, Alfarahidi University, Baghdad, Iraq, Email: alia.jasim@turath.edu.iq; Assoc. Prof. Dr. Noor Asniza Murad, School of Electrical Engineering, Universiti Teknologi Malaysia, Johor Bahru, Malaysia, Email: asniza@utm.my; Dr. Mona Riza Mohd Esa, School of Electrical Engineering, Universiti Teknologi Malaysia, Johor Bahru, Malaysia, Email: mona@utm.my; Yaqdhan Mahmood Hussein, Information Technology and Communication (ITC), Al-Furat Al-Awsat Technical University, Samawah, Iraq, Email: yaqthanm79@gmail.com

## REFERENCES

- [1] R. Shadid and S. Noghianian, "A Literature Survey on Wireless Power Transfer for Biomedical Devices," *Int. J. Antennas Propag.*, vol. 2018, 2018, doi: 10.1155/2018/4382841.
- [2] M. M. Soliman *et al.*, "Review on medical implantable antenna technology and imminent research challenges," *Sensors*, vol. 21, no. 9, 2021, doi: 10.3390/s21093163.
- [3] R. Alrawashdeh, "Patch antenna based on spiral split rings for bone implants," *Prz. Elektrotechniczny*, vol. 96, no. 7, pp. 129–134, 2020, doi: 10.15199/48.2020.07.24.
- [4] N. Dixit, A. Agarwal, and K. Patkar, "Implementation of multiple

- square slots in micro-strip rectangular patch antenna for S-band application," in *2016 Symposium on Colossal Data Analysis and Networking (CDAN)*, Mar. 2016, pp. 1–3, doi: 10.1109/CDAN.2016.7570931.
- [5] Z. Bao, Y. X. Guo, and R. Mittra, "Conformal Capsule Antenna with Reconfigurable Radiation Pattern for Robust Communications," *IEEE Trans. Antennas Propag.*, vol. 66, no. 7, pp. 3354–3365, 2018, doi: 10.1109/TAP.2018.2829828.
- [6] P. Loktongbam, D. Pal, and C. Koley, "Design of an implantable antenna for biotelemetry applications," *Microsyst. Technol.*, vol. 26, no. 7, pp. 2217–2226, 2020, doi: 10.1007/s00542-019-04531-y.
- [7] M. M. Jawad, N. N. A. Malik, N. A. Murad, M. R. Ahmad, M. R. M. Esa, and Y. M. Hussein, "Design of substrate integrated waveguide with minkowski-sierpinski fractal antenna for wlan applications," *Bull. Electr. Eng. Informatics*, vol. 9, no. 6, pp. 2455–2461, 2020, doi: 10.11591/eei.v9i6.2194.
- [8] S. Ahmad *et al.*, "A Wideband Bear-Shaped Compact Size Implantable Antenna for In-Body Communications," *Appl. Sci.*, vol. 12, no. 6, 2022, doi: 10.3390/app12062859.
- [9] O. Gürdoğan, A. E. Aydın, and S. C. Başaran, "Multilayered Implantable Antenna Design for Biotelemetry Communication," *Turkish J. Electromechanics Energy*, vol. 3, no. 1, pp. 1–5, 2018, [Online]. Available: <https://sloi.org/urn:sl:joee3167>.
- [10] J. Wang, M. Leach, E. G. Lim, Z. Wang, R. Pei, and Y. Huang, "An Implantable and Conformal Antenna for Wireless Capsule Endoscopy," *IEEE Antennas Wirel. Propag. Lett.*, vol. 17, no. 7, pp. 1153–1157, 2018, doi: 10.1109/LAWP.2018.2836392.
- [11] A. J. A. Al-Gburi *et al.*, "High Gain of UWB CPW-fed mercedes-shaped printed monopole antennas for UWB applications," *Prz. Elektrotechniczny*, vol. 97, no. 5, pp. 70–73, 2021, doi: 10.15199/48.2021.05.11.
- [12] M. S. Miah, A. N. Khan, C. Icheln, K. Haneda, and K. Takizawa, "Antenna Systems for Wireless Capsule Endoscope: Design, Analysis and Experimental Validation," pp. 1–11, 2018, [Online]. Available: <http://arxiv.org/abs/1804.01577>.
- [13] S. Hout and J. Y. Chung, "Design and Characterization of a Miniaturized Implantable Antenna in a Seven-Layer Brain Phantom," *IEEE Access*, vol. 7, no. November, pp. 162062–162069, 2019, doi: 10.1109/ACCESS.2019.2951489.
- [14] N. Ganeshwaran, J. K. Jeyaprakash, M. G. N. Alsath, and V. Sathyanarayanan, "Design of a Dual-Band Circular Implantable Antenna for Biomedical Applications," *IEEE Antennas Wirel. Propag. Lett.*, vol. 19, no. 1, pp. 119–123, 2020, doi: 10.1109/LAWP.2019.2955140.
- [15] F. Faisal, M. Zada, A. Ejaz, Y. Amin, S. Ullah, and H. Yoo, "A Miniaturized Dual-Band Implantable Antenna System for Medical Applications," *IEEE Trans. Antennas Propag.*, vol. 68, no. 2, pp. 1161–1165, 2020, doi: 10.1109/TAP.2019.2938591.
- [16] S. Symeonidis, W. G. Whittow, M. Zecca, and C. Panagamuwa, "Bone fracture monitoring using implanted antennas in the radius, tibia and phalange heterogeneous bone phantoms," *Biomed. Phys. Eng. Express*, vol. 4, no. 4, 2018, doi: 10.1088/2057-1976/aab974.
- [17] Z. Xia *et al.*, "A Wideband Circularly Polarized Implantable Patch Antenna for ISM Band Biomedical Applications," *IEEE Trans. Antennas Propag.*, vol. 68, no. 3, pp. 2399–2404, 2020, doi: 10.1109/TAP.2019.2944538.
- [18] S. Ahmad, B. Manzoor, S. Naseer, N. Santos-Valdivia, A. Ghaffar, and M. I. Abbasi, "X-Shaped Slotted Patch Biomedical Implantable Antenna for Wireless Communication Networks," *Wirel. Commun. Mob. Comput.*, vol. 2022, 2022, doi: 10.1155/2022/7594587.
- [19] D. Nikolayev, W. Joseph, A. Skrivervik, M. Zhadobov, L. Martens, and R. Sauleau, "Dielectric-Loaded Conformal Microstrip Antennas for Versatile In-Body Applications," *IEEE Antennas Wirel. Propag. Lett.*, vol. 18, no. 12, pp. 2686–2690, 2019, doi: 10.1109/LAWP.2019.2948814.
- [20] M. S. Singh, J. Ghosh, S. Ghosh, and A. Sarkhel, "Miniaturized Dual-Antenna System for Implantable Biotelemetry Application," *IEEE Antennas Wirel. Propag. Lett.*, vol. 20, no. 8, pp. 1394–1398, 2021, doi: 10.1109/LAWP.2021.3081477.
- [21] M. S. Miah, C. Icheln, M. M. Islam, and K. Haneda, "An Ultrawideband Conformal Antenna at 433 MHz for Wireless Capsule Endoscope of Pediatric Patients," *IEEE Int. Symp. Pers. Indoor Mob. Radio Commun. PIMRC*, vol. 2018-Sept, pp. 350–355, 2018, doi: 10.1109/PIMRC.2018.8580890.
- [22] M. R. Islam, R. R. Hasan, M. A. Haque, S. Ahmad, K. A. Mazed, and M. R. Islam, "In-body antenna for wireless capsule endoscopy at MICS band," *Adv. Intell. Syst. Comput.*, vol. 857, pp. 801–810, 2019, doi: 10.1007/978-3-030-01177-2\_59.
- [23] K. Chen, Q. Xu, X. Shen, and C. Ren, "The Effect of Zigzag Boundaries on the Reverberation Chamber Performance," *IEEE Access*, vol. 9, pp. 145471–145476, 2021, doi: 10.1109/ACCESS.2021.3123352.
- [24] H. Ullah and F. A. Tahir, "A broadband wire hexagon antenna array for future 5G communications in 28 GHz band," *Microw. Opt. Technol. Lett.*, vol. 61, no. 3, pp. 696–701, 2019, doi: 10.1002/mop.31613.
- [25] M. Takahashi, "Antennas for Wireless Power Transmission of Capsule Endoscope," *2018 IEEE Int. Work. Electromagn. Appl. Student Innov. Compet. IWEM 2018*, vol. 1, pp. 1–2, 2018, doi: 10.1109/IWEM.2018.8536724.
- [26] M. Sarestoniemi, C. Pomalaza-Raez, C. Kissi, and J. Iinatti, "Simulation and Measurement Data-Based Study on Fat as Propagation Medium in WBAN Abdominal Implant Communication Systems," *IEEE Access*, vol. 9, pp. 46240–46259, 2021, doi: 10.1109/ACCESS.2021.3068116.
- [27] P. Gas and A. Miaskowski, "SAR optimization for multi-dipole antenna array with regard to local hyperthermia," *Prz. Elektrotechniczny*, vol. 95, no. 1, pp. 17–20, 2019, doi: 10.15199/48.2019.01.05.
- [28] C. Liu, Y. X. Guo, and S. Xiao, "Capacitively loaded circularly polarized implantable patch antenna for ISM band biomedical applications," *IEEE Trans. Antennas Propag.*, vol. 62, no. 5, pp. 2407–2417, 2014, doi: 10.1109/TAP.2014.2307341.
- [29] L. J. Xu, Y. X. Guo, and W. Wu, "Miniaturized circularly polarized loop antenna for biomedical applications," *IEEE Trans. Antennas Propag.*, vol. 63, no. 3, pp. 922–930, 2015, doi: 10.1109/TAP.2014.2387420.
- [30] H. Li, Y. X. Guo, and S. Q. Xiao, "Broadband circularly polarized implantable antenna for biomedical applications," *Electron. Lett.*, vol. 52, no. 7, pp. 504–506, 2016, doi: 10.1049/el.2015.4445.
- [31] X. Y. Liu, Z. T. Wu, Y. Fan, and E. M. Tentzeris, "A Miniaturized CSRR Loaded Wide-Beamwidth Circularly Polarized Implantable Antenna for Subcutaneous Real-Time Glucose Monitoring," *IEEE Antennas Wirel. Propag. Lett.*, vol. 16, no. c, pp. 577–580, 2017, doi: 10.1109/LAWP.2016.2590477.
- [32] K. Zhang, C. Liu, X. Liu, H. Guo, and X. Yang, "Miniaturized Circularly Polarized Implantable Antenna for ISM-Band Biomedical Devices," *Int. J. Antennas Propag.*, vol. 2017, 2017, doi: 10.1155/2017/9750257.
- [33] C. Liu, Y. Zhang, and X. Liu, "Circularly Polarized Implantable Antenna for 915 MHz ISM-Band Far-Field Wireless Power Transmission," *IEEE Antennas Wirel. Propag. Lett.*, vol. 17, no. 3, pp. 373–376, 2018, doi: 10.1109/LAWP.2018.2790418.
- [34] N. Pournoori, S. Ma, L. Sydanheimo, L. Ukkonen, T. Bjorninen, and Y. Rahmat-Samii, "Compact dual-band PIFA based on a slotted radiator for wireless biomedical implants," *2019 IEEE Int. Symp. Antennas Propag. Usn. Radio Sci. Meet. APSURSI 2019 - Proc.*, no. October, pp. 13–14, 2019, doi: 10.1109/APUSNCURSINRSM.2019.8889083.
- [35] Y. Alamgir *et al.*, "Compacted Conformal Implantable Antenna with Multitasking Capabilities for Ingestible Capsule Endoscope," *IEEE Access*, vol. 8, pp. 157617–157627, 2020, doi: 10.1109/ACCESS.2020.3019663.
- [36] D. Nguyen and C. Seo, "An ultra-miniaturized antenna using loading circuit method for medical implant applications," *IEEE Access*, vol. 9, pp. 111890–111898, 2021, doi: 10.1109/ACCESS.2021.3103827.
- [37] K. Liu *et al.*, "Design of Conformal Spiral Dual-Band Antenna for Wireless Capsule System," *IEEE Access*, vol. PP, p. 1, 2021, doi: 10.1109/ACCESS.2021.3106735.
- [38] T. Le and T. Y. Yun, "Wearable Dual-Band High-Gain Low-SAR Antenna for Off-Body Communication," *IEEE Antennas Wirel. Propag. Lett.*, vol. 20, no. 7, pp. 1175–1179, 2021,